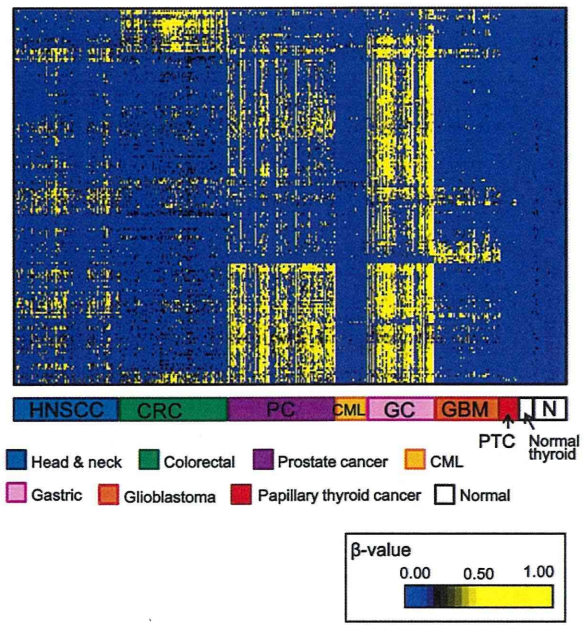

FIGURE 2 | Heatmap for methylation status of several cancer types. Genes with β-value <0.17 in normal samples and with standard deviation of β-value in cancer samples >0.15, were selected and their β-values were shown by heatmap. Each cancer type showed different methylation profile, and papillary thyroid cancer displayed fewer aberrantly methylated genes than other cancer types. HNSCC, head and neck squamous cell carcinoma; CRC, colorectal cancer; PC, prostate cancer; CML, chronic myeloid leukemia; GC, gastric cancer; GBM, glioblastoma; PTC, papillary thyroid cancer; N, normal samples corresponding to these cancer types.

node metastasis, distant metastasis, tumor stage, age, or sex, did not show significant difference.

To validate the methylation status of these genes, six out of the 25 genes, *HIST1H3J*, *POU4F2*, *SHOX2*, *PHKG2*, *TLX3*, and *HOXA7*, were randomly chosen and analyzed by pyrosequencing, a highly quantitative method (**Figure 4**). Although one normal sample showed high methylation in *POU4F2*, frequent hypermethylation of these genes in papillary cancer samples was confirmed, while normal thyroid samples were generally unmethylated.

EVALUATION OF GENE SILENCING

The analyzed tissue samples include a part of non-tumor cells (see Materials and Methods). To evaluate whether these aberrantly methylated genes were silenced in cancer cells, we analyzed methylation status of these six genes in papillary thyroid cancer cell lines (TPC1, KTC1, and KTC3) and anaplastic thyroid cancer cell line BHT-101 (**Figure 5A**). All the genes except *SHOX2* showed dense methylation in at least one papillary thyroid cancer cell line, confirming that hypermethylation detected in cancer tissue samples is due to hypermethylation in cancer cells.

We next performed real-time RT-PCR for the six genes. All the genes except *SHOX2* showed no or very low expression in the analyzed, methylated cancer cell line, and showed re-expression in cells treated with 5-aza-2′-deoxycytidine and/or trichostatin A (**Figure 5B**). *SHOX2* was neither expressed, nor methylated in KTC1 (**Figure 5A**). Consequently, its expression was not reversed by the deoxycytidine/trichostatin treatment (**Figure 5B**). This is presumably because *SHOX2* was silenced in KTC1 by mechanisms other than promoter methylation, e.g., by depletion of appropriate transcription factors.

METHYLATION ANALYSIS OF THE SIX GENES IN ADDITIONAL SAMPLES

To statistically extend the validation of aberrant methylation of the six genes, we analyzed the methylation status in 20 additional papillary thyroid cancer samples and 10 additional normal thyroid samples by pyrosequencing (**Figure 6**). A similar fraction of cancer samples showed high methylation in each gene (2/20 for *HIST1H3J*, 8/20 for *POU4F2*, 4/20 for *SHOX2*, 5/20 for *PHKG2*, 6/20 for *TLX3*, and 4/20 for *HOXA7*).

When methylation ratios were compared between 34 cancer samples in total and 20 normal samples in total, five genes (*HIST1H3J*, *SHOX2*, *PHKG2*, *TLX3*, and *HOXA7*) showed significantly higher methylation in cancer ($P < 0.05$, ranging from 0.0001 to 0.004, t-test), and *POU4F2* tended to show higher methylation in cancer ($P = 0.07$, t-test) (**Figure 7A**). Among the 34 cancer samples, 26 showed aberrant methylation in at least one gene, but eight showed no aberrant methylation at all (**Figure 7B**). When clinicopathological features were compared between methylation(+) cancer and methylation(−) cancer, mutations of *BRAF*/*RAS* oncogenes significantly correlated to methylation(+) groups ($P = 0.04$, Fisher's exact test) (**Table 4**). Although it was not statistically significant, methylation(+) cancer tended to show larger size of tumor ($P = 0.06$, t-test) and higher levels of thyroglobulin ($P = 0.08$, t-test).

DISCUSSION

In this study, we performed genome-wide DNA methylation analysis in 14 human papillary thyroid cancer samples and 10 normal samples. Although papillary thyroid cancer apparently involves fewer aberrantly methylated genes than other types of cancers, we detected 25 genes frequently hypermethylated in papillary thyroid cancer. Methylation status was quantitatively validated in six out of the 25 genes by pyrosequencing, using the genome-widely analyzed samples and additional samples. Gene silencing in papillary thyroid cancer cell lines was confirmed by real-time RT-PCR. While a subset of cancer cases had no aberrant methylation at all, cancer with preferential methylation tended to have oncogene mutation and to be larger tumor.

Papillary thyroid cancer displayed fewer aberrantly methylated genes, compared with other cancer types (**Figure 2**). For genes previously reported to be methylated in thyroid cancer, such as *TSHR* (Xing et al., 2003), or in other cancer types, such as *RASSF1A*, *RAR-β2*, *p16*, *CDH1*, *DAPK*, and *MLH1*, the methylation frequency in papillary thyroid cancer ranges from 15 to 33% (Hoque et al., 2005; Guan et al., 2008; Mohammadi-asl et al., 2011). In these reports, no or few normal samples were analyzed (Guan et al., 2008; Mohammadi-asl et al., 2011), methylation was also detected in normal samples (Hoque et al., 2005), or a non-quantitative method, i.e., standard methylation-specific

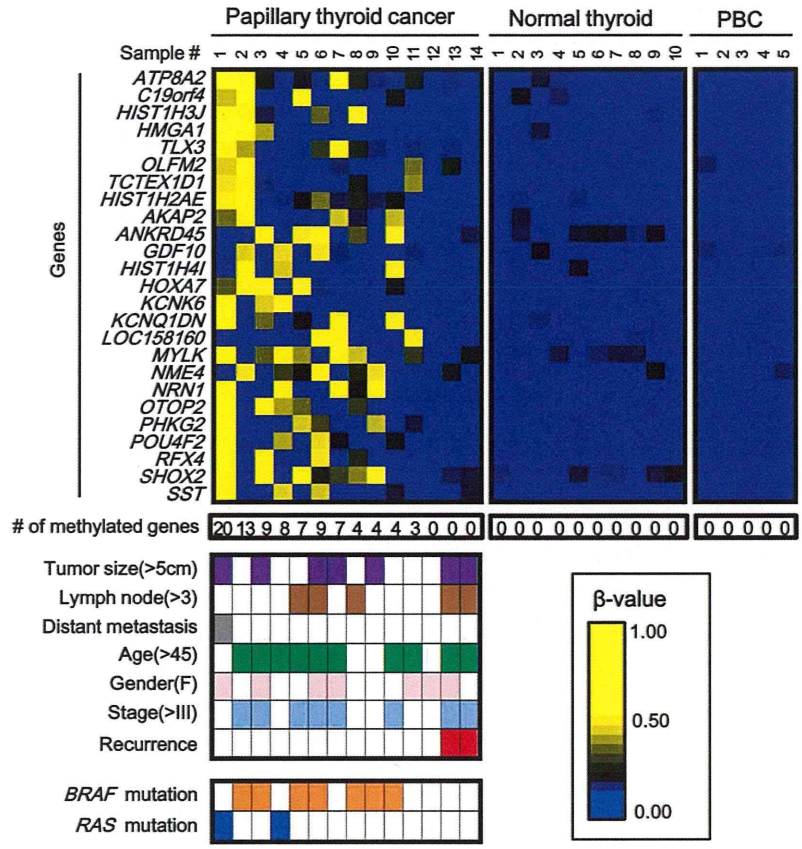

FIGURE 3 | Aberrantly methylated genes frequently observed in papillary thyroid cancer. PBC, peripheral blood cells. We detected 25 genes that were hypermethylated ($\beta > 0.25$) in at least three of 14 papillary thyroid cancer samples, but not methylated ($\beta < 0.2$) in 10 normal samples. Among the 14 papillary cancer samples, 11 showed aberrant methylation in three or more genes, whereas the other three samples had no aberrant methylation. Purple, tumor size; brown, number of metastatic lymph nodes >3; gray, distant metastasis(+); green, age over 45 years old; pink, female; pale blue, stage III or IV; red, recurrence (+); orange, *BRAF* mutation(+); blue, *RAS* mutation (+). The two samples with recurrence (red) had no aberrant methylation ($P = 0.03$, Fisher's exact test). *BRAF*/*RAS* oncogene mutations were all observed in methylation(+) samples ($P = 0.03$, Fisher's exact test).

PCR, was used (Guan et al., 2008). Standard methylation-specific PCR (Herman et al., 1996) can amplify and detect minor fraction of methylated alleles, but its high sensitivity can lead to overestimation of methylation frequency. Our analysis did not select these genes as frequently methylated ones in the first 14 cancer samples, because normal thyroid tissues also showed high methylation levels or because methylation frequencies in papillary thyroid cancer samples were low ($\leq$2 of 14 cancer samples). Instead, we detected 25 novel genes that were frequently aberrantly methylated ($\beta > 0.25$) in at least three of the 14 cancer samples, and not methylated in any of the 10 normal thyroid samples ($\beta < 0.2$).

Interestingly, three of the 14 papillary thyroid cancer samples showed no aberrant methylation in the 25 genes, but the other 11 cancer samples showed hypermethylation in at least three of the 25 genes. No cancer sample showed aberrant methylation in just one or two genes. This unusual distribution of aberrant methylation is similar to the CpG island methylator phenotype (CIMP), which was first proposed in colorectal cancer (Toyota et al., 1999). As Toyota et al. demonstrated in colorectal cancer (Toyota et al., 1999), we calculated probability of methylation distribution in papillary thyroid cancer using these 25 genes. The fraction of methylated tumors in each gene was 3/14 for *ATP8A2*, 3/14 for *C19orf4*, ..., 5/14 for *ANKRD45*, ..., 6/14 for *MYLK*, ..., 4/14 for *NRN1*, ..., 5/14 for *SHOX2*, and 3/14 for *SST* (**Figure 3**). Assuming that methylation of these genes is random, the probability that none of the 25 genes would be methylated in three cancer samples is $P = 1.2 \times 10^{-8}$. This was calculated using the following formula:

$$p(x) = \frac{\binom{N}{x}\prod_g \binom{N-x}{f(g)}}{\prod_g \binom{N}{f(g)}}$$

where x indicates number of samples which do not have methylated genes ($x = 3$ in the present case), N indicates number of cancer samples ($N = 14$ here), g indicates one of the 25 genes,

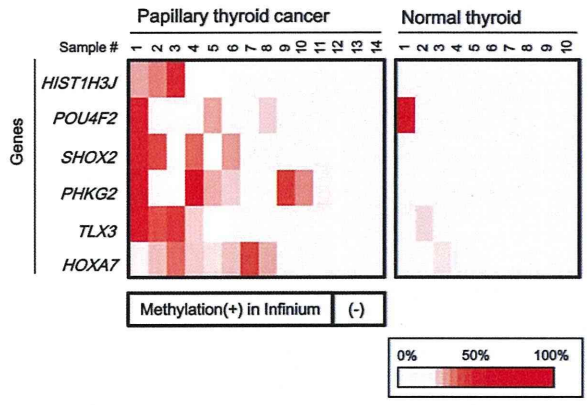

FIGURE 4 | Confirmation of aberrant methylation by pyrosequencing. Six genes were randomly chosen among the 25 frequently methylated genes, and their methylation status was quantitatively validated by pyrosequencing, using the 14 papillary thyroid cancer samples and 10 normal thyroid samples that were analyzed by Infinium. Although one normal sample showed high methylation in *POU4F2*, aberrant methylation of the six genes in the papillary cancer samples was confirmed. **Bottom**, the corresponding data for aberrant methylation obtained by Infinium analysis (**Figure 3**).

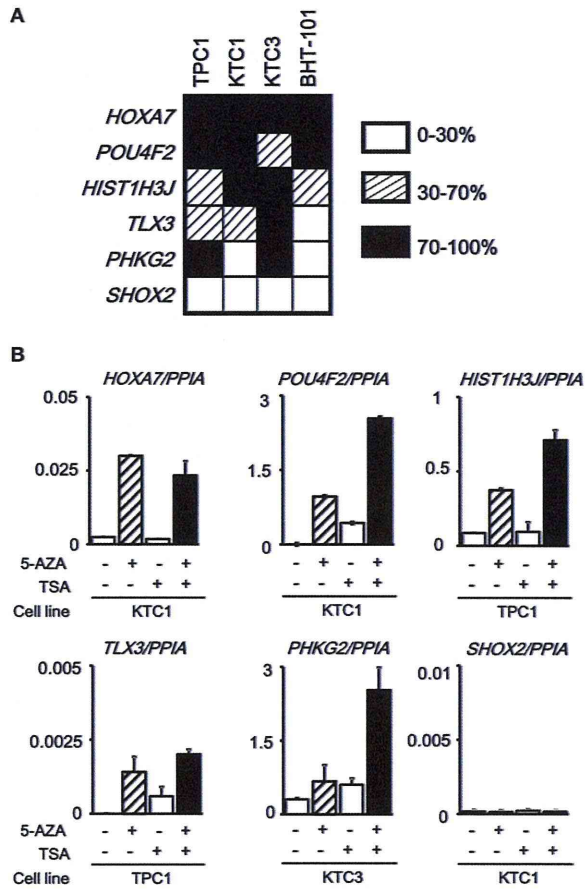

FIGURE 5 | Silencing of aberrantly methylated genes. (A) Methylation status of the *HOXA7, POU4F2, HIST1H3J, TLX3, PHKG2, SHOX2* genes was analyzed in papillary thyroid cancer cell lines TPC1, KTC1, and KTC3 and anaplastic thyroid cancer cell line BHT-101 by pyrosequencing. *Open box*, 0–30% methylation, presumably no allele methylation. *Hatched box*, 30–70% methylation, presumably hemi-allelic or partial methylation. *Closed box*, 70–100% methylation, presumably bi-allelic and dense methylation. All the genes except *SHOX2* showed dense methylation in at least one papillary thyroid cancer cell line. **(B)** Real-time RT-PCR analysis of the methylated genes. Cells were treated with 5-aza-2′-deoxycytidine (5-AZA) and/or trichostatin A (TSA). Gene expression levels were normalized to that of *PPIA* (*Peptidylprolyl Isomerase A*, or *cyclophilin A*). All the genes except *SHOX2* showed no or very low expression in the analyzed cancer cell line, and showed re-expression in cells treated with 5-AZA/TSA.

and $f(g)$ indicates the number of samples in which g is methylated. Similarly, the probability that at least three of the 25 genes are methylated in 11 cancer samples would be $P = 0.0028$. In each case, a random event is highly unlikely. We rather observe that the associated methylation or un-methylation events both occur at relatively high frequencies. Our data thus suggest that there are two distinct classes of papillary thyroid cancer. One is a subset of hardly methylated cancer. The second one is a subset of preferentially methylated cancer, prone to transcriptional silencing and with the potential to inactivate several genes simultaneously, as CIMP has been proposed in colorectal cancer and other cancers (Toyota et al., 1999; Kaneda et al., 2002; Noushmehr et al., 2010).

Although the number of analyzed samples was not large, preferentially methylated papillary thyroid cancer showed mutation of *BRAF/RAS* oncogenes more frequently than methylation(−) cancer ($P = 0.04$, Fisher's exact test). In previous studies of papillary thyroid cancer, although methylation of *RASSF1A* and *BRAF* mutation were detected in a mutually exclusive manner (Xing et al., 2004; Hoque et al., 2005), methylation of *RARβ2* or *MLH1* significantly correlated to *BRAF* mutation (Hoque et al., 2005; Guan et al., 2008). Correlation of aberrant methylation and oncogene mutation are also reported in colorectal cancer; high-methylation and intermediate-methylation epigenotypes strongly correlated to *BRAF* mutation and *KRAS* mutation, respectively, and low-methylation epigenotype strongly correlated to lack of oncogene mutation (Shen et al., 2007; Yagi et al., 2010; Hinoue et al., 2012). The mechanism of these correlations is still unknown, but oncogene mutation may somehow induce aberrant methylation, or aberrant methylation may help escape from senescence by disrupting factors critical in *RAF/RAS*-induced senescence (Kaneda and Yagi, 2011).

Preferentially methylated cancer also tended to have larger tumors and higher thyroglobulin levels, which might relate to cancer progression (Piccardo et al., 2013). Although 90% of papillary thyroid cancers are considered to be at low risk with a mortality rate of 1–2%, the mortality rate of the high risk group is 50–75% (Hay et al., 1993; Noguchi et al., 1994; Shaha et al., 1996; Dean and Hay, 2000). The tumor-node-metastasis (TNM) classification is a tool for cancer prognosis; each variable used in TNM staging (age, tumor size, extent of primary tumor, and presence of nodal or distant metastases) shows significant association with observed end points of cancer recurrence or death. Cancer

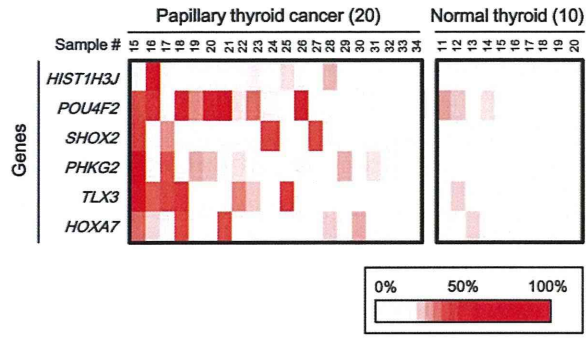

FIGURE 6 | Aberrant methylation of *HOXA7, POU4F2, HIST1H3J, TLX3, PHKG2, SHOX2* genes in additional samples: 20 cancer samples and 10 normal ones. Methylation status of the six genes was confirmed by pyrosequencing. Bottom, color scale with known methylation degrees (0–100%).

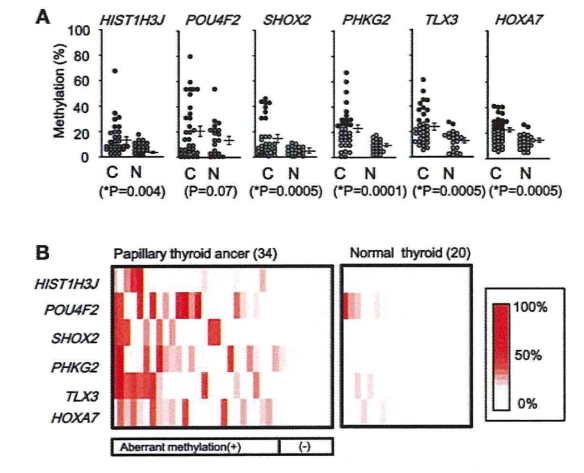

FIGURE 7 | Methylation status of the six genes in 54 samples analyzed by pyrosequencing. (A) Each gene was methylated to a different extent in each sample. *C*, 34 cancer samples. *N*, 20 normal samples. *Circle*, methylation ratio of each sample. Filled circles indicate that the gene is methylated with the methylation ratio >25%. *Bars*, the mean and standard error of methylation ratios. *P*-values were calculated by *t*-test to compare distribution of methylation ratios between cancer (*C*) and normal (*N*) samples. Five genes (*HIST1H3J, SHOX2, PHKG2, TLX3*, and *HOXA7*) showed significantly higher methylation in cancer ($P < 0.05$, *t*-test). *POU4F2* tended to show higher methylation in cancer ($P = 0.07$, *t*-test). **(B)** Heatmap for methylation status of the 54 analyzed samples. Among the 34 papillary thyroid cancer samples, 26 were aberrant methylation(+) in at least one of six genes, while eight had no methylation. In **Table 4**, the number of cancer samples with aberrant methylation ($n = 26$) and the number of samples without aberrant methylation ($n = 8$) refer to these data.

Table 4 | Aberrant methylation and clinicopathological features.

Clinical features	All Cases ($n = 34$)	Aberrant Methylation(+) ($n = 26$, Figure 7B)	Aberrant Methylation(−) ($n = 8$, Figure 7B)	*P*-values
SEX				
Male/female	11/23	10/16	1/7	0.17 (Fisher)
AGE (YEAR)				
Mean ± SE	56.0 ± 2.7	57.2 ± 3.1	52.4 ± 4.9	0.45 (*t*-test)
TUMOR SIZE (mm)				
Mean ± SE	26.2 ± 2.6	28.3 ± 3.3	20.1 ± 2.0	0.06 (*t*-test)
NUMBER OF LYMPH NODES WITH METASTASIS				
Mean ± SE	2.6 ± 0.7	2.2 ± 0.6	3.3 ± 1.6	0.53 (*t*-test)
DISTANT METASTASIS				
(+)/(−)	0/34	0/26	0/8	1 (Fisher)
RECURRENCE				
(+)/(−)	5/28	3/22	2/6	0.37 (Fisher)
Unknown	1	1	0	
THYROGLOBULIN (ng/ml)				
Mean ± SE	104.6 ± 52.1	129.3 ± 68.6	30.5 ± 9.3	0.08 (*t*-test)
MUTATION OF BRAF/RAS ONCOGENES				
(+)/(−)	26/7	22/3	4/4	0.04* (Fisher)
Unknown	1	1	0	

*SE, standard error. P-values were calculated to compare methylation(+) group and methylation(−) groups and to analyze the correlation of methylation status to clinicopathological features. Fisher, calculated by Fisher's exact test. t-test, calculated by t-test. *P < 0.05, which is considered as statistically significant. Mutations of BRAF/RAS oncogenes are thus considered to correlate significantly with methylation(+) groups.*

recurrence and mortality ratios are significantly lower in stage I (15.4% and 1.7%, respectively) compared with more advanced tumors (22% and 15.8% in stage II, 46.4% and 30% in stage III, and 66.7% and 60.9% in stage IV, respectively) (Loh et al., 1997). Molecular diagnostic markers are still not used, although their development is anticipated (McLeod et al., 2013). Although aberrant methylation was not significantly associated with lymph node metastasis, distant metastasis, or recurrence in analysis of the 34 cancer samples in this study, further study should be performed using larger set of clinical samples for comparison of aberrant methylation, gene mutation status, and prognosis.

As for detected genes, *TLX3* (*HOX11L2*) is a transcription factor highly expressed in T-cell leukemia (Baak et al., 2008), and its aberrant methylation was observed in cisplatin-resistant bladder cancer (Tada et al., 2011). *SHOX2* is a member of the homeobox gene family, and is reported to relate to a short-stature phenotype of Turner syndrome (Clement-Jones et al., 2000). DNA methylation of *SHOX2* was suggested to be a biomarker for diagnosis of lung cancer based on bronchial aspirates (Schmidt et al., 2010). *HOXA7* is also a transcription factor belonging to the homeobox gene family that regulates gene expression, morphogenesis, and differentiation (La Celle and Polakowska, 2001). *POU4F2* is one of POU family genes with Pit-Oct-Unc domain, and is a transcription factor with a role in cell identity and regulation

of nerve cell or retinal development (Weishaupt et al., 2005). PHKG2 is the gamma subunit of phosphorylase kinase, containing the active site of the enzyme. Phosphorylase kinase-deficient liver glycogenosis can be caused by mutations of phosphorylase kinase subunits, *PHKA2*, *PHKB*, or *PHKG2*, but *PHKG2* mutation was reported to cause a severe phenotype of this disease (Burwinkel et al., 2003). *HIST1H3J* encodes a member of histone H3 family, and is found in the small histone gene cluster on chromosome 6p22-p21.3 (NCBI gene data bank). If the role of histone modifications is known to affect the regulation of gene expression, less is known about the possible direct involvement of histones, an H3 variant in the present case, in thyroid tumorigenesis. Further investigation is necessary to clarify tumorigenic roles of these genes and their methylation, in papillary thyroid cancer and other types of cancer (Schmidt et al., 2010; Tada et al., 2011).

In summary, 25 new genes were found to be frequently methylated in papillary thyroid cancer. There might be subsets of papillary thyroid cancer hardly methylated and preferentially methylated, and aberrant methylation of these genes correlates *a priori* to *BRAF/RAS* oncogene mutation in papillary thyroid cancer.

AUTHOR CONTRIBUTIONS

Yasuko Kikuchi, Koichi Yagi, and Keisuke Matsusaka performed the experiments. Eiichi Tsuji and Toshihisa Ogawa prepared clinical samples and information. Junichi Kurebayashi established and supplied cell lines. Yasuko Kikuchi, Shingo Tsuji and Atsushi Kaneda analyzed and interpreted the data. Yasuko Kikuchi and Atsushi Kaneda wrote the manuscript. Toshihisa Ogawa, Hiroyuki Aburatani, and Atsushi Kaneda supervised the study.

ACKNOWLEDGMENTS

We thank Dr. Mitsutake, University of Nagasaki, for kindly providing cancer cell line TPC-1, and Hiroko Meguro, Kyoko Fujinaka and Kaori Nakano for their technical help. This work was supported by Grants-in-Aid for Scientific Research from the Ministry of Education, Culture, Sports, Science and Technology of Japan, and by JST CREST program.

REFERENCES

Baak, U., Gokbuget, N., Orawa, H., Schwartz, S., Hoelzer, D., Thiel, E., et al. (2008). Thymic adult T-cell acute lymphoblastic leukemia stratified in standard- and high-risk group by aberrant HOX11L2 expression: experience of the German multicenter ALL study group. *Leukemia* 22, 1154–1160. doi: 10.1038/leu.2008.52

Baylin, S. B., Ohm, J. E. (2006). Epigenetic gene silencing in cancer - a mechanism for early oncogenic pathway addiction. *Nat. Rev. Cancer* 6, 107–116. doi: 10.1038/nrc1799

Burwinkel, B., Rootwelt, T., Kvittingen, E. A., Chakraborty, P. K., and Kilimann, M. W. (2003). Severe phenotype of phosphorylase kinase-deficient liver glycogenosis with mutations in the PHKG2 gene. *Pediatr. Res.* 54, 834–839. doi: 10.1203/01.PDR.0000088069.09275.10

Clement-Jones, M., Schiller, S., Rao, E., Blaschke, R. J., Zuniga, A., Zeller, R., et al. (2000). The short stature homeobox gene SHOX is involved in skeletal abnormalities in Turner syndrome. *Hum. Mol. Genet.* 9, 695–702. doi: 10.1093/hmg/9.5.695

Cohen, Y., Xing, M., Mambo, E., Guo, Z., Wu, G., Trink, B., et al. (2003). BRAF mutation in papillary thyroid carcinoma. *J. Natl. Cancer Inst.* 95, 625–627. doi: 10.1093/jnci/95.8.625

Dean, D. S., and Hay, I. D. (2000). Prognostic indicators in differentiated thyroid carcinoma. *Cancer Control* 7, 229–239.

Esteller, M. (2007). Cancer epigenomics: DNA methylomes and histone-modification maps. *Nat. Rev. Genet.* 8, 286–298. doi: 10.1038/nrg2005

Ezaki, H., Ebihara, S., Fujimoto, Y., Iida, F., Ito, K., Kuma, K., et al. (1992). Analysis of thyroid carcinoma based on material registered in Japan during 1977-1986 with special reference to predominance of papillary type. *Cancer* 70, 808–814. doi: 10.1002/1097-0142(19920815)70:4<808::AID-CNCR2820700415>3.0.CO;2-L

Feinberg, A. P., Ohlsson, R., and Henikoff, S. (2006). The epigenetic progenitor origin of human cancer. *Nat. Rev. Genet.* 7, 21–33. doi: 10.1038/nrg1748

Guan, H., Ji, M., Hou, P., Liu, Z., Wang, C., Shan, Z., et al. (2008). Hypermethylation of the DNA mismatch repair gene hMLH1 and its association with lymph node metastasis and T1799A BRAF mutation in patients with papillary thyroid cancer. *Cancer* 113, 247–255. doi: 10.1002/cncr.23548

Hay, I. D., Bergstralh, E. J., Goellner, J. R., Ebersold, J. R., and Grant, C. S. (1993). Predicting outcome in papillary thyroid carcinoma: development of a reliable prognostic scoring system in a cohort of 1779 patients surgically treated at one institution during 1940 through 1989. *Surgery* 114, 1050–1057. discussion: 7–8.

Herman, J. G., Graff, J. R., Myohanen, S., Nelkin, B. D., and Baylin, S. B. (1996). Methylation-specific PCR: a novel PCR assay for methylation status of CpG islands. *Proc. Natl. Acad. Sci. U.S.A.* 93, 9821–9826. doi: 10.1073/pnas.93.18.9821

Hinoue, T., Weisenberger, D. J., Lange, C. P., Shen, H., Byun, H. M., Van Den Berg, D., et al. (2012). Genome-scale analysis of aberrant DNA methylation in colorectal cancer. *Genome Res.* 22, 271–282. doi: 10.1101/gr.117523.110

Hoque, M. O., Rosenbaum, E., Westra, W. H., Xing, M., Ladenson, P., Zeiger, M. A., et al. (2005). Quantitative assessment of promoter methylation profiles in thyroid neoplasms. *J. Clin. Endocrinol. Metab.* 90, 4011–4018. doi: 10.1210/jc.2005-0313

Ishizaka, Y., Itoh, F., Tahira, T., Ikeda, I., Ogura, T., Sugimura, T., et al. (1989). Presence of aberrant transcripts of ret proto-oncogene in a human papillary thyroid carcinoma cell line. *Jpn. J. Cancer Res.* 80, 1149–1152. doi: 10.1111/j.1349-7006.1989.tb01645.x

Jemal, A., Murray, T., Ward, E., Samuels, A., Tiwari, R. C., Ghafoor, A., et al. (2005). Cancer statistics, 2005. *CA. Cancer J. Clin.* 55, 10–30. doi: 10.3322/canjclin.55.1.10

Joo, J. Y., Park, J. Y., Yoon, Y. H., Choi, B., Kim, J. M., Jo, Y. S., et al. (2012). Prediction of occult central lymph node metastasis in papillary thyroid carcinoma by preoperative BRAF analysis using fine-needle aspiration biopsy: a prospective study. *J. Clin. Endocrinol. Metab.* 97, 3996–4003. doi: 10.1210/jc.2012-2444

Kaneda, A., Kaminishi, M., Yanagihara, K., Sugimura, T., and Ushijima, T. (2002). Identification of silencing of nine genes in human gastric cancers. *Cancer Res.* 62, 6645–6650.

Kaneda, A., and Yagi, K. (2011). Two groups of DNA methylation markers to classify colorectal cancer into three epigenotypes. *Cancer Sci.* 102, 18–24. doi: 10.1111/j.1349-7006.2010.01712.x

Kimura, E. T., Nikiforova, M. N., Zhu, Z., Knauf, J. A., Nikiforov, Y. E., and Fagin, J. A. (2003). High prevalence of BRAF mutations in thyroid cancer: genetic evidence for constitutive activation of the RET/PTC-RAS-BRAF signaling pathway in papillary thyroid carcinoma. *Cancer Res.* 63, 1454–1457.

Knauf, J. A., and Fagin, J. A. (2009). Role of MAPK pathway oncoproteins in thyroid cancer pathogenesis and as drug targets. *Curr. Opin. Cell Biol.* 21, 296–303. doi: 10.1016/j.ceb.2009.01.013

Kondo, T., Nakazawa, T., Murata, S., Kurebayashi, J., Ezzat, S., Asa, S. L., et al. (2007). Enhanced B-Raf protein expression is independent of V600E mutant status in thyroid carcinomas. *Hum. Pathol.* 38, 1810–1818. doi: 10.1016/j.humpath.2007.04.014

Kurebayashi, J., Okubo, S., Yamamoto, Y., Ikeda, M., Tanaka, K., Otsuki, T., et al. (2006). Additive antitumor effects of gefitinib and imatinib on anaplastic thyroid cancer cells. *Cancer Chemother. Pharmacol.* 58, 460–470. doi: 10.1007/s00280-006-0185-x

Kurebayashi, J., Tanaka, K., Otsuki, T., Moriya, T., Kunisue, H., Uno, M., et al. (2000). All-trans-retinoic acid modulates expression levels of thyroglobulin and cytokines in a new human poorly differentiated papillary thyroid carcinoma cell line, KTC-1. *J. Clin. Endocrinol. Metab.* 85, 2889–2896. doi: 10.1210/jc.85.8.2889

La Celle, P. T., and Polakowska, R. R. (2001). Human homeobox HOXA7 regulates keratinocyte transglutaminase type 1 and inhibits differentiation. *J. Biol. Chem.* 276, 32844–32853. doi: 10.1074/jbc.M104598200

Lee, K. C., Li, C., Schneider, E. B., Wang, Y., Somervell, H., Krafft, M., et al. (2012). Is BRAF mutation associated with lymph node metastasis in patients with papillary thyroid cancer. *Surgery* 152, 977–983. doi: 10.1016/j.surg.2012.08.019

Loh, K. C., Greenspan, F. S., Gee, L., Miller, T. R., and Yeo, P. P. (1997). Pathological tumor-node-metastasis (pTNM) staging for papillary and follicular thyroid carcinomas: a retrospective analysis of 700 patients. *J. Clin. Endocrinol. Metab.* 82, 3553–3562. doi: 10.1210/jc.82.11.3553

Matsusaka, K., Kaneda, A., Nagae, G., Ushiku, T., Kikuchi, Y., Hino, R., et al. (2011). Classification of Epstein-Barr virus-positive gastric cancers by definition of DNA methylation epigenotypes. *Cancer Res.* 71, 7187–7197. doi: 10.1158/0008-5472.CAN-11-1349

McLeod, D. S., Sawka, A. M., and Cooper, D. S. (2013). Controversies in primary treatment of low-risk papillary thyroid cancer. *Lancet* 381, 1046–1057. doi: 10.1016/S0140-6736(12)62205-3

Mitsutake, N., Miyagishi, M., Mitsutake, S., Akeno, N., Mesa, C. Jr., Knauf, J. A., et al. (2006). BRAF mediates RET/PTC-induced mitogen-activated protein kinase activation in thyroid cells: functional support for requirement of the RET/PTC-RAS-BRAF pathway in papillary thyroid carcinogenesis. *Endocrinology* 147, 1014–1019. doi: 10.1210/en.2005-0280

Mohammadi-asl, J., Larijani, B., Khorgami, Z., Tavangar, S. M., Haghpanah, V., Kheirollahi, M., et al. (2011). Qualitative and quantitative promoter hypermethylation patterns of the P16, TSHR, RASSF1A and RARbeta2 genes in papillary thyroid carcinoma. *Med. Oncol.* 28, 1123–1128. doi: 10.1007/s12032-010-9587-z

Nagae, G., Isagawa, T., Shiraki, N., Fujita, T., Yamamoto, S., Tsutsumi, S., et al. (2011). Tissue-specific demethylation in CpG-poor promoters during cellular differentiation. *Hum. Mol. Genet.* 20, 2710–2721. doi: 10.1093/hmg/ddr170

Namba, H., Nakashima, M., Hayashi, T., Hayashida, N., Maeda, S., Rogounovitch, T. I., et al. (2003). Clinical implication of hot spot BRAF mutation, V599E, in papillary thyroid cancers. *J. Clin. Endocrinol. Metab.* 88, 4393–4397. doi: 10.1210/jc.2003-030305

Noguchi, S., Murakami, N., and Kawamoto, H. (1994). Classification of papillary cancer of the thyroid based on prognosis. *World J. Surg.* 18, 552–7. discussion: 8. doi: 10.1007/BF00353763

Noushmehr, H., Weisenberger, D. J., Diefes, K., Phillips, H. S., Pujara, K., Berman, B. P., et al. (2010). Identification of a CpG island methylator phenotype that defines a distinct subgroup of glioma. *Cancer Cell* 17, 510–522. doi: 10.1016/j.ccr.2010.03.017

Piccardo, A., Arecco, F., Puntoni, M., Foppiani, L., Cabria, M., Corvisieri, S., et al. (2013). Focus on high-risk DTC patients: high postoperative serum thyroglobulin level is a strong predictor of disease persistence and is associated to progression-free survival and overall survival. *Clin. Nucl. Med.* 38, 18–24. doi: 10.1097/RLU.0b013e318266d4d8

Schmidt, B., Liebenberg, V., Dietrich, D., Schlegel, T., Kneip, C., Seegebarth, A., et al. (2010). SHOX2 DNA methylation is a biomarker for the diagnosis of lung cancer based on bronchial aspirates. *BMC Cancer* 10:600. doi: 10.1186/1471-2407-10-600

Shaha, A. R., Shah, J. P., and Loree, T. R. (1996). Risk group stratification and prognostic factors in papillary carcinoma of thyroid. *Ann. Surg. Oncol.* 3, 534–538. doi: 10.1007/BF02306085

Shen, L., Toyota, M., Kondo, Y., Lin, E., Zhang, L., Guo, Y., et al. (2007). Integrated genetic and epigenetic analysis identifies three different subclasses of colon cancer. *Proc. Natl. Acad. Sci. U.S.A.* 104, 18654–18659. doi: 10.1073/pnas.0704652104

Suzuki, H., Gabrielson, E., Chen, W., Anbazhagan, R., van Engeland, M., Weijenberg, M. P., et al. (2002). A genomic screen for genes upregulated by demethylation and histone deacetylase inhibition in human colorectal cancer. *Nat. Genet.* 31, 141–149. doi: 10.1038/ng892

Tada, Y., Yokomizo, A., Shiota, M., Tsunoda, T., Plass, C., and Naito, S. (2011). Aberrant DNA methylation of T-cell leukemia, homeobox 3 modulates cisplatin sensitivity in bladder cancer. *Int. J. Oncol.* 39, 727–733. doi: 10.3892/ijo.2011.1049

Toyota, M., Ahuja, N., Ohe-Toyota, M., Herman, J. G., Baylin, S. B., and Issa, J. P. (1999). CpG island methylator phenotype in colorectal cancer. *Proc. Natl. Acad. Sci. U.S.A.* 96, 8681–8686. doi: 10.1073/pnas.96.15.8681

Ulisse, S., Baldini, E., Sorrenti, S., Barollo, S., Prinzi, N., Catania, A., et al. (2012). In papillary thyroid carcinoma BRAFV600E is associated with increased expression of the urokinase plasminogen activator and its cognate receptor, but not with disease-free interval. *Clin. Endocrinol. (Oxf.)* 77, 780–786. doi: 10.1111/j.1365-2265.2012.04465.x

Vogel, N., Schiebel, K., and Humeny, A. (2009). Technologies in the whole-genome age: MALDI-TOF-based genotyping. *Transfus. Med. Hemother.* 36, 253–262. doi: 10.1159/000225089

Weber, M., Hellmann, I., Stadler, M. B., Ramos, L., Paabo, S., Rebhan, M., et al. (2007). Distribution, silencing potential and evolutionary impact of promoter DNA methylation in the human genome. *Nat. Genet.* 39, 457–466. doi: 10.1038/ng1990

Weishaupt, J. H., Klocker, N., and Bahr, M. (2005). Axotomy-induced early down-regulation of POU-IV class transcription factors Brn-3a and Brn-3b in retinal ganglion cells. *J. Mol. Neurosci.* 26, 17–25. doi: 10.1385/JMN:26:1:017

Xing, M., Cohen, Y., Mambo, E., Tallini, G., Udelsman, R., Ladenson, P. W., et al. (2004). Early occurrence of RASSF1A hypermethylation and its mutual exclusion with BRAF mutation in thyroid tumorigenesis. *Cancer Res.* 64, 1664–1668. doi: 10.1158/0008-5472.CAN-03-3242

Xing, M., Haugen, B. R., and Schlumberger, M. (2013). Progress in molecular-based management of differentiated thyroid cancer. *Lancet* 381, 1058–1069. doi: 10.1016/S0140-6736(13)60109-9

Xing, M., Usadel, H., Cohen, Y., Tokumaru, Y., Guo, Z., Westra, W. B., et al. (2003). Methylation of the thyroid-stimulating hormone receptor gene in epithelial thyroid tumors: a marker of malignancy and a cause of gene silencing. *Cancer Res.* 63, 2316–2321.

Xing, M., Westra, W. H., Tufano, R. P., Cohen, Y., Rosenbaum, E., Rhoden, K. J., et al. (2005). BRAF mutation predicts a poorer clinical prognosis for papillary thyroid cancer. *J. Clin. Endocrinol. Metab.* 90, 6373–6379. doi: 10.1210/jc.2005-0987

Yagi, K., Akagi, K., Hayashi, H., Nagae, G., Tsuji, S., Isagawa, T., et al. (2010). Three DNA methylation epigenotypes in human colorectal cancer. *Clin. Cancer Res.* 16, 21–33. doi: 10.1158/1078-0432.CCR-09-2006

Yagi, K., Takahashi, H., Akagi, K., Matsusaka, K., Seto, Y., Aburatani, H., et al. (2012). Intermediate methylation epigenotype and its correlation to KRAS mutation in conventional colorectal adenoma. *Am. J. Pathol.* 180, 616–625. doi: 10.1016/j.ajpath.2011.10.010

Yamashita, H., Noguchi, S., Murakami, N., Watanabe, S., Uchino, S., Kawamoto, H., et al. (1998). Changing trends and prognoses for patients with papillary thyroid cancer. *Arch. Surg.* 133, 1058–1065. doi: 10.1001/archsurg.133.10.1058

Conflict of Interest Statement: The authors declare that the research was conducted in the absence of any commercial or financial relationships that could be construed as a potential conflict of interest.

Received: 21 September 2013; accepted: 18 November 2013; published online: 05 December 2013.

Citation: Kikuchi Y, Tsuji E, Yagi K, Matsusaka K, Tsuji S, Kurebayashi J, Ogawa T, Aburatani H and Kaneda A (2013) Aberrantly methylated genes in human papillary thyroid cancer and their association with BRAF/RAS mutation. Front. Genet. 4:271. doi: 10.3389/fgene.2013.00271

This article was submitted to Epigenomics and Epigenetics, a section of the journal Frontiers in Genetics.

Mutational Analysis Reveals the Origin and Therapy-Driven Evolution of Recurrent Glioma

Brett E. Johnson *et al.*

Science **343**, 189 (2014);
DOI: 10.1126/science.1239947

progenitors express *bnl>GFP*. As progenitors continue along the DT, DT larval cells activate *bnl>GFP* expression one segment at a time from anterior to posterior, matching progenitor movement.

This dynamic *bnl* expression along the migration path is required for progenitor outgrowth. Knockdown of *bnl* expression by RNA interference (RNAi) in larval tracheal cells blocked migration and resulted in diminished or absent PAT (Fig. 3, B and C; fig. S7, A to C; and movie S2). Mosaic expression of *bnl RNAi* in small patches along the path (*23*) also arrested migration, so long as the patch encompassed the full DT circumference (Fig. 3D; fig. S7, D and E; and movies S3 and S4). Thus, Bnl is required all along the migration path, and the signal does not cross even short gaps.

Ectopic *bnl* expression in GFP-labeled clones of larval tracheal cells induced by *dfr-FLP* (*23*) redirected progenitor migration. Depending on the location of the clones, ectopic *bnl* caused incorrect exit from the niche, premature entry onto the DT, or wrong turns on the DT (Fig. 4, B to D). Dual clones induced bifurcation with groups of progenitors moving toward each ectopic *bnl* source (Fig. 4E). Clones in Tr3 and posterior metameres caused progenitors in these regions to leave the niche, even though they do not normally do so (Fig. 4, G and H, and fig. S8, D and E). When there was a large clone, progenitors migrated throughout the clone (Fig. 4F), implying that progenitors do not require a gradient and will spread to cover an entire region of cells expressing *bnl* at equivalent levels. When *bnl*-expressing clones failed to induce migration, the clones appeared to be too far from the progenitors or there was competition from another clone close by (fig. S8, A and B). Ectopic *bnl* expression within the progenitor cluster arrested migration (fig. S8C).

The results show that the embryonic tracheal inducer Bnl FGF guides tracheal progenitors out of the niche and into the posterior during tracheal metamorphosis. The source of Bnl is the larval tracheal branches destined for destruction, which serve both as the source of the chemoattractant and as the substratum for progenitor migration. Several days earlier in embryos, these larval tracheal branches were themselves induced by Bnl provided by neighboring tissues. But after embryonic development, most tracheal cells, including those in the decaying larval branches, downregulate *btl* FGFR expression (fig. S2A) and thus do not respond to (or sequester) the Bnl signal they later express. One of the most notable aspects of this larval Bnl is its exquisitely specific pattern in decaying larval branches, which presages progenitor outgrowth. It is unclear how Bnl expression is controlled, though it does not appear to require signals from migrating progenitors because the *bnl* reporter expression front progressed normally when progenitor outgrowth was stalled by a tracheal break (fig. S6C). Perhaps expression of Bnl involves gradients in the tracheal system or spatial patterning cues established during embryonic development in conjunction with temporal signals mediated by molting hormones.

Because the signal guiding progenitor migration is provided by tracheae destined for destruction, progenitors become positioned along the larval branches they replace (Fig. 4I). Perhaps during tissue repair and homeostasis, recruitment of adult stem or progenitor cells from the niche is similarly guided by signals from decaying tissue, thereby ensuring that new tissue is directed to the appropriate sites.

References and Notes

1. N. Barker, S. Bartfeld, H. Clevers, *Cell Stem Cell* **7**, 656–670 (2010).
2. G. B. Adams, D. T. Scadden, *Nat. Immunol.* **7**, 333–337 (2006).
3. A. Alvarez-Buylla, D. A. Lim, *Neuron* **41**, 683–686 (2004).
4. C. Blanpain, E. Fuchs, *Nat. Rev. Mol. Cell Biol.* **10**, 207–217 (2009).
5. E. Sancho, E. Batlle, H. Clevers, *Curr. Opin. Cell Biol.* **15**, 763–770 (2003).
6. G. L. Ming, H. Song, *Neuron* **70**, 687–702 (2011).
7. E. Nacu, E. M. Tanaka, *Annu. Rev. Cell Dev. Biol.* **27**, 409–440 (2011).
8. K. D. Poss, *Nat. Rev. Genet.* **11**, 710–722 (2010).
9. T. Matsuno, *Jap. J. Appl. Entomol. Zool.* **34**, 165–167 (1990).
10. G. Manning, M. A. Krasnow, in *The Development of* Drosophila melanogaster, M. Bate, A. Martinez-Arias, Eds. (Cold Spring Harbor Laboratory Press, Woodbury, NY, 1993), vol. 1, pp. 609–685.
11. M. Weaver, M. A. Krasnow, *Science* **321**, 1496–1499 (2008).
12. A. Guha, L. Lin, T. B. Kornberg, *Proc. Natl. Acad. Sci. U.S.A.* **105**, 10832–10836 (2008).
13. C. Pitsouli, N. Perrimon, *Development* **137**, 3615–3624 (2010).
14. M. Sato, Y. Kitada, T. Tabata, *Dev. Biol.* **318**, 247–257 (2008).
15. C. Ribeiro, M. Neumann, M. Affolter, *Curr. Biol.* **14**, 2197–2207 (2004).
16. L. Liu, W. A. Johnson, M. J. Welsh, *Proc. Natl. Acad. Sci. U.S.A.* **100**, 2128–2133 (2003).
17. K. Guillemin *et al.*, *Development* **122**, 1353–1362 (1996).
18. C. Klämbt, L. Glazer, B. Z. Shilo, *Genes Dev.* **6**, 1668–1678 (1992).
19. M. Reichman-Fried, B. Z. Shilo, *Mech. Dev.* **52**, 265–273 (1995).
20. D. Sutherland, C. Samakovlis, M. A. Krasnow, *Cell* **87**, 1091–1101 (1996).
21. J. Jarecki, E. Johnson, M. A. Krasnow, *Cell* **99**, 211–220 (1999).
22. M. Sato, T. B. Kornberg, *Dev. Cell* **3**, 195–207 (2002).
23. Materials and methods are available as supporting material on *Science* Online.
24. S. Hayashi *et al.*, *Genesis* **34**, 58–61 (2002).

Acknowledgments: We thank M. Weaver, M. Metzstein, and other lab members for advice and reagents. This work was supported by a Genentech Graduate Fellowship and a Ruth L. Kirschstein NIH training grant (F.C.) and the Howard Hughes Medical Institute.

Supplementary Materials

www.sciencemag.org/content/343/6167/186/suppl/DC1
Materials and Methods
Figs. S1 to S10
References (*25–39*)
Movies S1 to S4

4 June 2013; accepted 12 November 2013
10.1126/science.1241442

Mutational Analysis Reveals the Origin and Therapy-Driven Evolution of Recurrent Glioma

Brett E. Johnson,[1]* Tali Mazor,[1]* Chibo Hong,[1] Michael Barnes,[2] Koki Aihara,[3,4] Cory Y. McLean,[1]† Shaun D. Fouse,[1] Shogo Yamamoto,[3] Hiroki Ueda,[3] Kenji Tatsuno,[3] Saurabh Asthana,[5,6] Llewellyn E. Jalbert,[7] Sarah J. Nelson,[7,8] Andrew W. Bollen,[2] W. Clay Gustafson,[9] Elise Charron,[10] William A. Weiss,[1,9,10] Ivan V. Smirnov,[1] Jun S. Song,[11,12] Adam B. Olshen,[6,11] Soonmee Cha,[1] Yongjun Zhao,[13] Richard A. Moore,[13] Andrew J. Mungall,[13] Steven J. M. Jones,[13] Martin Hirst,[13] Marco A. Marra,[13] Nobuhito Saito,[4] Hiroyuki Aburatani,[3] Akitake Mukasa,[4] Mitchel S. Berger,[1] Susan M. Chang,[1] Barry S. Taylor,[5,6,11]‡ Joseph F. Costello[1]‡

Tumor recurrence is a leading cause of cancer mortality. Therapies for recurrent disease may fail, at least in part, because the genomic alterations driving the growth of recurrences are distinct from those in the initial tumor. To explore this hypothesis, we sequenced the exomes of 23 initial low-grade gliomas and recurrent tumors resected from the same patients. In 43% of cases, at least half of the mutations in the initial tumor were undetected at recurrence, including driver mutations in *TP53*, *ATRX*, *SMARCA4*, and *BRAF*; this suggests that recurrent tumors are often seeded by cells derived from the initial tumor at a very early stage of their evolution. Notably, tumors from 6 of 10 patients treated with the chemotherapeutic drug temozolomide (TMZ) followed an alternative evolutionary path to high-grade glioma. At recurrence, these tumors were hypermutated and harbored driver mutations in the RB (retinoblastoma) and Akt-mTOR (mammalian target of rapamycin) pathways that bore the signature of TMZ-induced mutagenesis.

The genetic landscape of tumors is continually evolving, which can be an impediment to the clinical management of cancer patients with recurrent disease (*1*, *2*). In contrast to the clonal evolution of hematological malignancies (*3*, *4*) and solid tumor metastases (*5–7*), the local regrowth of solid tumors after surgery occurs under a unique set of evolutionary pressures, which are further affected by adjuvant therapies. Through the acquisition of new mutations, residual tumor cells can progress to a more aggressive state. Grade II astrocytic gliomas are

particularly troublesome from this perspective. Although surgery is the standard of care, these invasive brain tumors typically recur (*8*). Many remain grade II at recurrence, while others progress to a higher histological grade with a poor prognosis (*9*). The incidence and timing of malignant progression are variable and unpredictable (*8*).

We undertook genome sequence analysis of initial and recurrent human gliomas to address two questions: (i) What is the extent to which mutations in initial tumors differ from their subsequent recurrent tumors? (ii) How does chemotherapy with temozolomide (TMZ), a drug commonly used in the treatment of glioma, affect the mutational profile of recurrent tumors? We sequenced the exomes of 23 grade II gliomas at initial diagnosis and their recurrences resected from the same patients up to 11 years later (table S1). We selected initial tumors of predominantly astrocytic histology that capture the full spectrum of glioma progression (histological grade II to IV at recurrence) and adjuvant treatment history. Tumor and matched normal DNA were sequenced to an average 125-fold coverage, enabling the sensitive detection of mutations down to a 10% variant frequency, small insertions and deletions, and DNA copy number alterations (CNAs) (Fig. 1A and tables S2 and S3) (*10*).

We identified an average of 33 somatic coding mutations in each initial tumor, of which an average of 54% were also detected at recurrence (shared mutations) (Fig. 1A). The shared mutations included those in *IDH1*, *TP53*, and *ATRX* in most but not all cases (fig. S1) (*11*–*13*). All other somatic mutations were identified only in the initial tumor or only in the recurrent tumor from a given patient (private mutations) and thus presumably arose later in tumor evolution. For example, mutations in *SMARCA4* were private to the initial or recurrent tumor in six of seven patients and therefore may confer a selective advantage in the context of preexisting early driver events (*14*, *15*). Overall, the initial and recurrent gliomas displayed a broad spectrum of genetic relatedness (fig. S2 and table S4). At one end of this spectrum were four patients whose tumors showed a pattern of linear clonal evolution; we infer that the recurrent tumors in these patients were seeded by cells bearing ≥75% of the mutations detected in the initial tumors (as in patient 27, Fig. 1B). At the other end of the spectrum, tumors from three patients showed branched clonal evolution; we infer that the recurrent tumors in these patients were seeded by cells derived from the initial tumor at an early stage of its evolution, as the recurrent tumors shared ≤25% of mutations detected in the initial tumors. Patient 17 was an extreme example of branched clonal evolution, as the initial and recurrent tumors shared only the *IDH1* R132H ($Arg^{132} \rightarrow His$) mutation (Fig. 1C). This further implicates *IDH1* mutations as an initiating event in low-grade gliomagenesis (*12*). Indeed, *IDH1* mutation was the only shared mutation in every patient—an observation that supports the current interest in IDH1 as a therapeutic target (*16*). Paired tumors from the remaining 16 patients formed a continuum between linear and branched clonal evolution. Together, these data illustrate the extent to which genetically similar low-grade gliomas diverge after surgical resection, and suggest that recurrences may emerge from early stages in the evolution of the initial tumor.

Many solid tumors, including glioblastoma (GBM), display intratumoral heterogeneity (*17*, *18*). For example, geographically distinct parts of the tumor may have different mutations. Intratumoral heterogeneity could be a confounding factor in estimates of genetic divergence when only one relatively small fraction of a tumor is sampled. To explore the extent of intratumoral heterogeneity in our cases, we first analyzed the *BRAF* V600E ($Val^{600} \rightarrow Glu$) mutation that was subclonal in the initial tumor of patient 18 and undetectable in the recurrent tumor by either exome sequencing or droplet digital polymerase chain reaction (PCR) (Fig. 1D and fig. S3) (*10*). *BRAF* V600E was present in three of six additional samples from geographically distinct regions of the initial tumor, whereas seven additional samples of the recurrence all lacked this mutation. These results suggest that the *BRAF*-mutant clone did not expand, despite the proliferative advantage typically conferred by this mutation. Such a finding contrasts sharply with the selection and outgrowth of subclonal drivers during the evolution of chronic lymphocytic leukemias (*3*).

Beyond the actionable *BRAF* mutation, we sequenced the exomes of additional, geographically distinct samples from three cases to further determine the extent to which apparently private mutations might be misclassified because of intratumoral heterogeneity. In patient 17, for whom all mutations except *IDH1* were private, intratumoral heterogeneity was observed in the initial and recurrent tumor. From the mutational profiles, however, we inferred that three samples of the initial tumor and four samples of the recurrence all derived from a common tumor cell of origin that possessed only an *IDH1* R132H mutation (Fig. 2A and table S5). Moreover, the recurrent tumor contained driver mutations in *TP53* and *ATRX* distinct from those observed in the initial tumor. We found no evidence of these new *TP53* or *ATRX* mutations in the initial tumor at allele frequencies of ~0.1% (figs. S3 and S4), implying convergent phenotypic evolution (*5*) via a strong ongoing selection for loss of these genes. The initial and recurrent tumors likely did not arise independently, as they also shared three somatic noncoding mutations (fig. S5). Thus, the initial and recurrent tumors were only distantly related and, despite the local and relatively rapid recurrence (fig. S6), exonic mutations other than *IDH1* R132H were only transiently present during the course of this patient's disease. Finally, we sequenced the exomes of additional distinct samples of the initial and recurrent tumors from patients 26 and 27, broadening our assessment of the impact of intratumoral heterogeneity on the reported genetic divergence. We found that only a small minority of private mutations were actually shared events (7%; table S3) (*10*). Intratumoral heterogeneity therefore could not explain the majority of the genetic divergence between the initial and recurrent tumors in our cohort, including the driver mutations in initial tumors that were undetected in their recurrence.

To investigate whether sequential recurrences from a single patient could each be traced to the same evolutionary stage of the initial tumor, we sequenced the exomes of the second and third recurrent tumors from patient 04 and constructed a disease phylogeny by clonal ordering (Fig. 2B, fig. S7, and table S5) (*5*, *19*). The initial tumor and three sequential local recurrences were clonally related, as indicated by the shared phylogenetic branch containing early driver mutations in *IDH1* and *TP53*. We infer that the tumor cells seeding the second recurrence branched off from the initial tumor at a slightly earlier evolutionary stage than the cells seeding the first recurrence. In contrast, the third recurrent tumor was a direct outgrowth of the second recurrence. These results show that branched and linear patterns of clonal evolution occurred at differing times in the same patient and are therefore not intrinsic properties of the tumor.

Beyond maximal, safe, surgical resection, there is currently no standard of care for patients with low-grade glioma; options include surveillance, adjuvant radiation alone, TMZ alone, or radiation and TMZ. TMZ is an alkylating agent that induces apoptosis in glioma cells and is sometimes used to defer or delay the use of radiation. However, there is currently no information on whether treatment of grade II astrocytomas with TMZ confers longer overall survival (*8*). Because TMZ is also mutagenic (*20*), we sought to determine how adjuvant chemotherapy with TMZ affects the mutational profile of recurrent tumors by comparing the initial low-grade gliomas to their recurrence after treatment. Although the initial tumors and most of the recurrent tumors in our cohort had 0.2 to 4.5 mutations per megabase (Mb) (*21*, *22*), 6 of the 10 patients treated with

[1]Department of Neurological Surgery, University of California, San Francisco, CA 94158, USA. [2]Department of Pathology, University of California, San Francisco, CA 94158, USA. [3]Genome Science Laboratory, Research Center for Advanced Science and Technology, University of Tokyo, Meguro-ku, Tokyo 153-8904, Japan. [4]Department of Neurosurgery, University of Tokyo, Bunkyo-ku, Tokyo 113-8655, Japan. [5]Department of Medicine, University of California, San Francisco, CA 94158, USA. [6]Helen Diller Family Comprehensive Cancer Center, University of California, San Francisco, CA 94158, USA. [7]Department of Bioengineering and Therapeutic Sciences, University of California, San Francisco, CA 94158, USA. [8]Department of Radiology and Biomedical Imaging, University of California, San Francisco, CA 94158, USA. [9]Department of Pediatrics, University of California, San Francisco, CA 94158, USA. [10]Department of Neurology, University of California, San Francisco, CA 94158, USA. [11]Department of Epidemiology and Biostatistics, University of California, San Francisco, CA 94158, USA. [12]Institute for Human Genetics, University of California, San Francisco, CA 94158, USA. [13]Michael Smith Genome Sciences Centre, British Columbia Cancer Agency, Vancouver, BC V5Z 4E6, Canada.

*These authors contributed equally to this work.
†Present address: 23andMe Inc., Mountain View, CA 94043, USA.
‡Corresponding author. E-mail: jcostello@cc.ucsf.edu (J.F.C.); barry.taylor@ucsf.edu (B.S.T.)

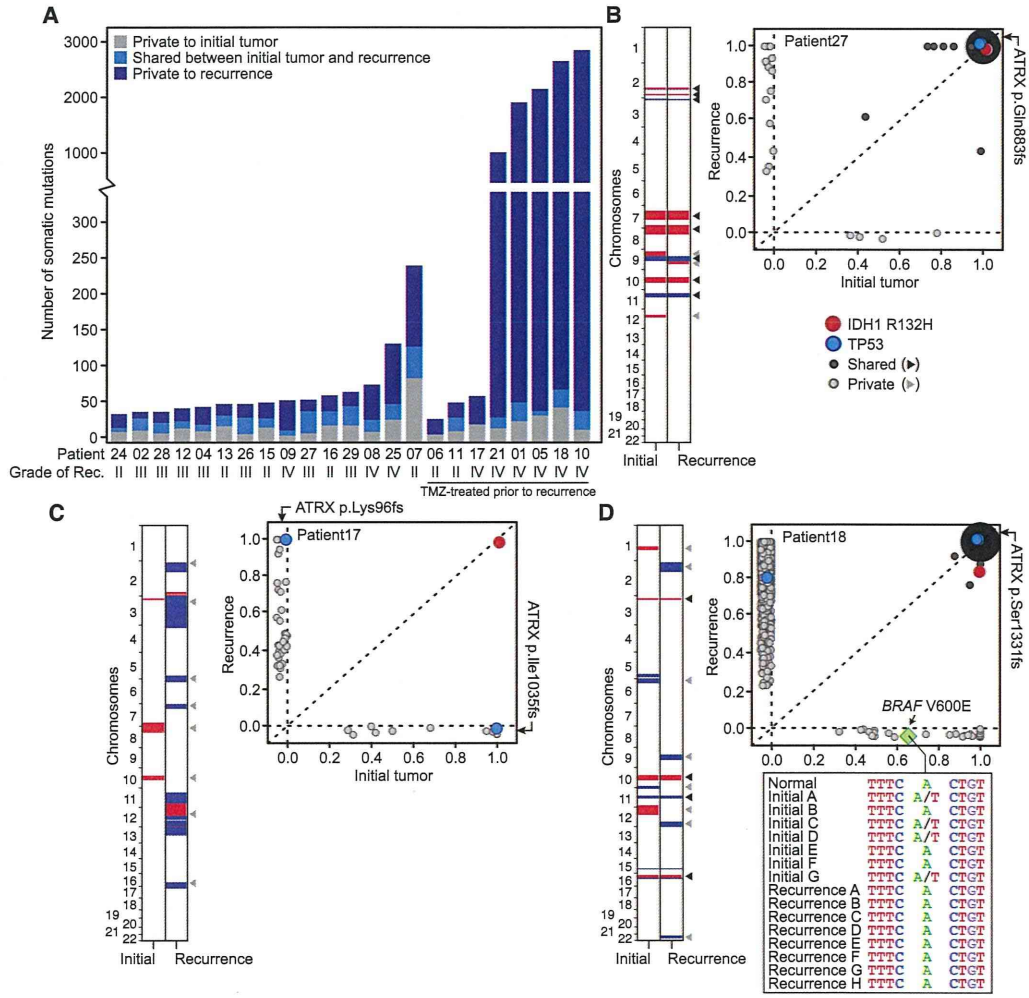

Fig. 1. Genetic landscapes of low-grade gliomas and their patient-matched recurrences. (**A**) Total number of mutations private to or shared between the initial and first recurrent glioma of 23 patients. (**B** to **D**) Shared and private somatic mutations in paired initial and recurrent tumors (*x* and *y* axes, respectively) as a function of the estimated fraction of tumor cells carrying the mutant allele. Mutations present in all the cells in both tumors are represented by a single point whose radius is scaled by the log count of such mutations. Shared and private CNAs are indicated (red and blue are gains and losses, respectively; white is copy-neutral). In (C), clonal *TP53* and *ATRX* mutations in the initial tumor were not identified in the recurrent tumor, but different clonal mutations in these two genes were acquired. (D) Inset shows the DNA sequence encompassing *BRAF* V600E in the normal tissue and in 15 geographically distinct samples of the initial and recurrent tumors.

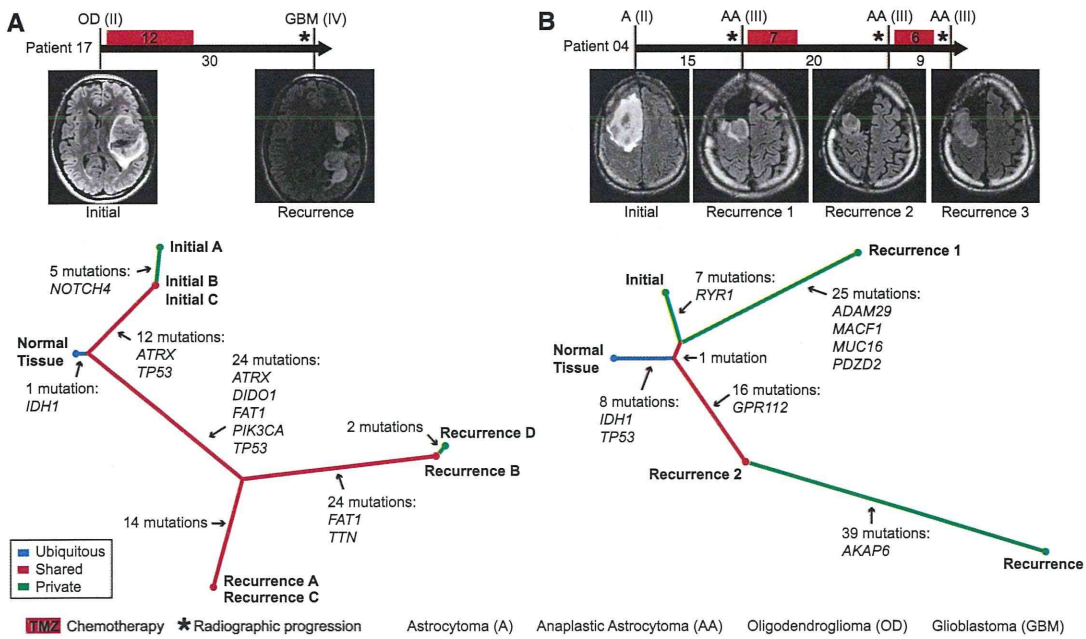

Fig. 2. Temporal and spatial patterns of clonal evolution in the tumors of two glioma patients. (**A** and **B**) A timeline of treatment histories for patient 17 (A) and patient 04 (B) (top, intervals labeled in months). Vertical bars correspond to the time of tumor resection and are labeled with the tumor diagnosis and grade. Representative MRIs are also shown. A phylogenetic tree (bottom) depicts the patterns of clonal evolution of these tumors inferred from the pattern and frequency of somatic mutations, highlighting genes frequently mutated in cancer.